

# PERFORMANCE OF SUPER-EXPONENTIAL ALGORITHM FOR BLIND EQUALIZATION

Chong-Yung Chi, Chih-Chun Feng and Ching-Yung Chen

Department of Electrical Engineering  
National Tsing Hua University, Hsinchu, Taiwan, R.O.C.  
Tel: 886-3-5731156, Fax: 886-3-5751787, E-mail: cychi@ee.nthu.edu.tw

**Abstract** - Shalvi and Weinstein proposed a computationally efficient iterative super-exponential algorithm (SEA) using higher-order cumulants for blind equalization. For practical situations of finite signal-to-noise ratio (SNR) and channels allowed to have zeros on the unit circle, it can be shown that the linear equalizer obtained using the SEA is stable with a nonlinear relation to the nonblind minimum mean square error (MMSE) equalizer, that it is a perfect phase equalizer for some cumulant orders, and that it is the same as the linear equalizer associated with Shalvi and Weinstein's blind deconvolution criteria for some cumulant orders. Then some simulation results are presented to justify the analytic results followed by some conclusions.

## I. Introduction

Blind equalization (deconvolution) is a crucial signal processing procedure to mitigate the multipath fading and noise effects of communication channels with only measurements given by

$$\begin{aligned} x[n] &= u[n] * h[n] + w[n] \\ &= \sum_{k=-\infty}^{\infty} h[k]u[n-k] + w[n] \end{aligned} \quad (1)$$

where  $h[n]$  is an unknown linear time-invariant (LTI) channel,  $u[n]$  is the transmitted signal and  $w[n]$  is additive noise. The linear equalizer, denoted by  $v[n]$ , has been widely used to process  $x[n]$  such that

$$e[n] = x[n] * v[n] = u[n] * g[n] + w[n] * v[n] \quad (2)$$

approximates  $\alpha u[n - \tau]$  where  $\alpha$  is a scale factor and  $\tau$  is a time delay, and

$$g[n] = h[n] * v[n] \quad (3)$$

This work was supported by the National Science Council under Grant NSC-89-2213-E-007-093.

is the (combined) overall system after equalization. Let  $\text{cum}\{x_1, \dots, x_p\}$  denote the  $p$ th-order joint cumulant of random variables  $x_1, \dots, x_p$  and

$$\text{cum}\{e[n] : p, \dots\} = \text{cum}\{x_1 = e[n], \dots, x_p = e[n], \dots\}.$$

Shalvi and Weinstein [1, 2] find the equalizer  $v[n]$  by maximizing the following criteria:

$$J_{p,q}(v[n]) = \frac{|\text{cum}\{e[n] : p, e^*[n] : q\}|}{[\text{cum}\{e[n], e^*[n]\}]^{(p+q)/2}}, \quad p+q \geq 3 \quad (4)$$

where the superscript '\*' denotes complex conjugation. Shalvi and Weinstein [2, 3] also proposed an iterative super-exponential algorithm (SEA) for blind equalization. The equalizer associated with  $J_{p,q}$  and the one associated with the SEA have been shown to be a zero-forcing equalizer (perfect equalization) when signal-to-noise ratio (SNR) equals infinity and the channel  $h[n]$  does not have zeros on the unit circle (i.e., the stable inverse filter of  $h[n]$  exists).

In practical applications, however, the SNR is always finite and the channel's zeros may be close to or exactly on the unit circle. Feng and Chi [4, 5] recently reported performance analyses for the optimum linear equalizer associated with  $J_{p,q}$  under these practical conditions, including its connection with the nonblind minimum mean square error (MMSE) equalizer [6], the stability property and perfect phase equalization property. In this paper, the performance of the linear equalizer associated with the SEA is analyzed including some properties and its relation to the MMSE equalizer and the one associated with  $J_{p,q}$ .

## II. Brief Review of SEA

Assume that we are given a set of measurements  $x[n]$  modeled as (1) under the following assumptions:

- (A1) The channel  $h[n]$  is stable (i.e.,  $\sum_n |h[n]| < \infty$ ) with frequency response  $H(\omega) = 0$  for  $\omega \in \Omega_Z \subset [-\pi, \pi]$ , i.e.,  $\Omega_Z = \{\omega | H(\omega) = 0, -\pi \leq \omega < \pi\}$ .

- (A2) The signal  $u[n]$  is a zero-mean, independent identically distributed (i.i.d.), non-Gaussian random process with variance  $\sigma_u^2$  and nonzero cumulant  $\mu_{p,q} = \text{cum}\{u[n] : p, u^*[n] : q\}$  where  $p + q \geq 3$ .
- (A3) The noise  $w[n]$  is zero-mean, white Gaussian with variance  $\sigma_w^2 > 0$  (finite SNR) and statistically independent of  $u[n]$ .

Moreover, the equalizer  $v[n]$  is assumed to be an FIR filter over the interval  $L_1 \leq n \leq L_2$  with length  $L = L_2 - L_1 + 1$ . Let

$$\mathbf{v} = [v[L_1], v[L_1 + 1], \dots, v[L_2]]^T.$$

At the  $i$ th iteration, the SEA [2, 3, 7] updates  $\mathbf{v}$  by

$$\mathbf{v}_i = \frac{\mathbf{R}_{xx}^{-1} \mathbf{d}_{ex}}{\|\mathbf{R}_{xx}^{-1} \mathbf{d}_{ex}\|} \quad (5)$$

where  $\mathbf{R}_{xx}$  is an  $L \times L$  correlation matrix of  $x[n]$  with the  $(k, l)$ th element given by

$$[\mathbf{R}_{xx}]_{k,l} = r_{xx}[k-l] = \text{cum}\{x[n-l], x^*[n-k]\} \quad (6)$$

and  $\mathbf{d}_{ex}$  is an  $L \times 1$  vector with the  $k$ th element given by

$$[\mathbf{d}_{ex}]_k = \text{cum}\{e_{i-1}[n] : p, e_{i-1}^*[n] : q-1, x^*[n-k']\} \quad (7)$$

in which  $k' = k + L_1 - 1$  and

$$e_{i-1}[n] = x[n] * v_{i-1}[n] \quad (8)$$

is the equalized signal obtained at the  $(i-1)$ th iteration. As the SEA converges, the linear equalizer  $v[n]$  associated with  $\mathbf{v}_i$  is obtained and  $e[n] = e_i[n]$  is the obtained equalized signal. Let us conclude this section with the following remark:

- (R1) The SEA is computational efficient because of its fast convergence (at a super-exponential rate) and only computing the linear equations given by (5) at each iteration.

### III. Performance Analysis of SEA

Without confusion, let  $v[n]$  denote the linear equalizer obtained by the SEA algorithm. It can be easily shown that as the SEA converges, the linear equations given by (5) without normalization are equivalent to the following linear equations

$$\begin{aligned} \sum_{l=L_1}^{L_2} r_{xx}[k-l] \cdot v[l] &= r_{xx}[k] * v[k] \\ &= \text{cum}\{e[n] : p, e^*[n] : q-1, x^*[n-k]\} \end{aligned}$$

$$\begin{aligned} &= \mu_{p,q} \sum_m g^p[m] (g^*[m])^{q-1} h^*[m-k] \\ &= \mu_{p,q} d[k] * h^*[-k], \quad k = L_1, \dots, L_2 \end{aligned} \quad (9)$$

where

$$d[k] = g^p[k] (g^*[k])^{q-1} \quad (10)$$

Let us further assume that  $L_1 = -\infty$  and  $L_2 = \infty$  and  $\sum_n |v[n]|^2 < \infty$  for investigating behaviors of  $v[n]$  based on (9). Taking Fourier transform of both sides of (9) with respect to  $k$  leads to the following two properties.

**Property 1.** The linear equalizer  $V(\omega)$  is related to the noncausal MMSE equalizer  $V_{\text{MSE}}(\omega)$  [6] via

$$V(\omega) = \beta \cdot D(\omega) V_{\text{MSE}}(\omega) \quad (11)$$

where  $\beta$  is a nonzero constant,  $D(\omega)$  is the Fourier transform of  $d[k]$  given by (10), and

$$V_{\text{MSE}}(\omega) = \frac{\sigma_u^2 \cdot H^*(\omega)}{\sigma_u^2 \cdot |H(\omega)|^2 + \sigma_w^2} \quad (12)$$

**Property 2.** Both  $v[n]$  and the associated overall system  $g[n]$  are always stable regardless of  $\Omega_Z = \emptyset$  or  $\Omega_Z \neq \emptyset$ , and meanwhile  $V(\omega) = G(\omega) = 0 \forall \omega \in \Omega_Z$ .

Property 1 also implies that  $v[n]$  is usually not a perfect amplitude equalizer (i.e.,  $|V(\omega)| \neq \alpha/|H(\omega)|$ ). However, it can be a perfect phase equalizer, i.e.,

$$\arg[V(\omega)] = -\arg[H(\omega)] - \omega\tau + \kappa, \quad -\pi \leq \omega < \pi \quad (13)$$

for some choices of  $p$  and  $q$  as given in the following property, where  $\tau$  and  $\kappa$  are constants.

**Property 3.** The linear equalizer  $V(\omega)$  is a perfect phase equalizer as given by (13) for two cases: (a)  $x[n]$  is real for all  $p + q \geq 3$  and (b)  $x[n]$  is complex and  $p = q \geq 2$ .

The Property 3 can be proved by the observation that  $g[n]$  and  $d[n]$  have the same phase by (11), i.e.,  $d[n] * g^*[-n]$  is zero-phase. However, for the case that  $x[n]$  is complex and  $p \neq q$ , we empirically found that  $V(\omega)$  can be a perfect phase equalizer for most applications. Property 3 also implies that the choice of  $p = q = 2$  is preferable to other choices of  $p$  and  $q$  when the SEA is employed to process complex measurements.

In addition to the relation between the linear equalizer  $v[n]$  associated with the SEA and the MMSE equalizer  $v_{\text{MSE}}[n]$  as presented in Property 1, the former is also related to the linear equalizer, denoted by  $\nu[n]$ , associated with  $J_{p,q}$  as given in the following fact:

**Fact 1.** Feng and Chi [5, 7] have shown that  $\nu[n]$  also shares the Property 1 with  $d[k]$  different from the one

given by (10), and meanwhile it is a perfect phase equalizer for all  $p + q \geq 3$  regardless of whether  $x[n]$  is real or complex. However, for the two cases mentioned in Property 3,  $d[k]$  is the same for both  $v[n]$  and  $\nu[n]$ , and therefore  $v[n] = \alpha\nu[n - \tau]$  for these two cases.

With finite data, the optimum  $\nu[n]$  of finite length is usually obtained through an iterative gradient-type optimization procedure for finding the maximum of the highly nonlinear objective function  $J_{p,q}$ . Fact 1 suggests an efficient optimization algorithm making use of the SEA for finding the optimum  $\nu[n]$  for the two cases presented in Property 3 as follows:

**Algorithm 1:**

At the  $i$ th iteration,  $\nu_i = [\nu_i[L_1], \nu_i[L_1+1], \dots, \nu_i[L_2]]^T$  is obtained through the following two steps.

- (T1) Update  $\mathbf{v}_i$  by (5) that is also equal to  $\partial J_{p,q}/\partial \nu$  for  $\nu = \nu_{i-1}$  [2].
- (T2) If  $J_{p,q}(v_i[n]) > J_{p,q}(\nu_{i-1}[n])$ , update  $\nu_i[n] = v_i[n]$ , otherwise update  $\nu_i[n]$  through a gradient-type optimization with the gradient obtained in (T1).

Note that compared with gradient type algorithms, fast convergence and significant computational saving of Algorithm 1 can be expected because it shares the computational efficiency of the SEA as mentioned in (R1). To verify the preceding analytic results, the following FFT based iterative algorithm based on Property 1 is proposed for obtaining the theoretical (true)  $v[n]$ , up to a scale factor and a time delay, from  $h[n]$  and  $V_{\text{MSE}}(\omega)$ .

**Algorithm 2:**

- (S1) Set  $i = 0$ . Choose an initial guess  $v^{[0]}[n]$  for  $v[n]$ .
- (S2) Set  $i = i + 1$ . Compute  $g^{[i-1]}[n] = h[n] * v^{[i-1]}[n]$  by (3) and

$$g[n] = \frac{g^{[i-1]}[n]}{g^{[i-1]}[n_0]}$$

where  $n_0 = \arg \max\{|g^{[i-1]}[n]|, \forall n\}$ .

- (S3) Compute  $d[n]$  by (10) and its  $M$ -point DFT  $D(\omega_k) = 2\pi k/M$  using FFT.
- (S4) Compute  $\tilde{V}(\omega_k) = D(\omega_k) \cdot V_{\text{MSE}}(\omega_k)$  by (11) and its  $M$ -point inverse DFT  $\tilde{v}[n]$  using FFT followed by

$$v^{[i]}[n] = \frac{\tilde{v}[n]}{(\sum_n |\tilde{v}[n]|^2)^{1/2}}$$

- (S5) If  $\sum_n |v^{[i]}[n] - v^{[i-1]}[n]|^2 > \epsilon$  (a preassigned tolerance for convergence), then go to (S2); otherwise, the true  $v[n] = v^{[i]}[n]$  is obtained.

## IV. Simulation Results

The source signal  $u[n]$  was assumed to be a 4-QAM signal and the channel  $h[n] = h_1[n] * h_2[n]$  taken from [5] was used where  $h_1[n]$  and  $h_2[n]$  were causal FIR filters with coefficients  $\{1, 0, -1\}$  and  $\{0.04, -0.05, 0.07, -0.21, -0.5, 0.72, 0.36, 0, 0.21, 0.03, 0.07\}$ , respectively. The channel's magnitude response  $|H(\omega)|$  and phase response  $\text{ARG}[H(\omega)]$  are displayed in Figures 1(a) and 1(b), respectively. Note that phase discontinuities of  $\pi$  at  $\omega \in \Omega_z = \{0, -\pi\}$  can be observed due to the two zeros of  $H(z)$  at  $z = \pm 1$ .

The synthetic data  $x[n]$  were generated for data length  $N = 8000$  and SNR = 10 dB (complex white Gaussian noise). The equalizer  $\hat{v}[n]$  assumed to be a thirtieth-order ( $L = 31$ ) causal FIR filter was then obtained by the SEA with  $p = q = 2$  and  $\hat{v}_0[n] = \delta[n - 15]$ . Meanwhile the equalizer  $\hat{v}[n]$ , of the same order as  $\hat{v}[n]$ , associated with  $J_{2,2}$  was obtained using Algorithm 1 and a gradient-type optimization algorithm with  $\hat{v}_0[n] = \delta[n - 15]$ . Thirty independent runs were performed, and then the averages  $\hat{v}_{\text{ave}}[n]$  and  $\hat{v}[n]$  of the obtained 30 estimates  $\hat{v}[n]$  and  $\hat{v}[n]$  were calculated, respectively. On the other hand, the true  $v[n]$  was obtained using Algorithm 2 with initial condition  $v^{[0]}[n] = \delta[n]$ , DFT length  $M = 1024$  and  $\epsilon = 10^{-5}$ .

Real parts, magnitude responses and phase responses of the obtained  $\hat{v}_{\text{ave}}[n]$  (dash lines) and  $v[n]$  (dotted lines) are shown in Figures 2(a), 2(b) and 2(c), respectively, where time delays between  $\hat{v}_{\text{ave}}[n]$  and  $v[n]$  were artificially removed. Their imaginary parts are not displayed since they are almost zero. One can see, from these figures, that  $\hat{v}_{\text{ave}}[n]$  and  $V_{\text{ave}}(\omega)$  are almost indistinguishable from  $v[n]$  and  $V(\omega)$ , respectively. These results verify the preceding Properties 1, 2 and 3 and the efficacy of Algorithm 2.

The simulation results for  $\hat{v}[n]$  obtained using Algorithm 1 corresponding to those for  $\hat{v}[n]$  shown in Figures 2(a) through 2(c) are shown in Figures 3(a) through 3(c), respectively. The results shown in the former and those shown in the latter are very close to each other, and thus Fact 1 is justified and Algorithm 1 is effective. Moreover, the same results as shown in Figure 3(a) through 3(c) can also be obtained only using the gradient-type algorithm. Figure 3(d) shows the average of the thirty  $J_{2,2}$ 's with respect to iteration number associated with Algorithm 1 (solid line) and that associated with the gradient-type algorithm (dash line). One can see, from Figure 3(d), that, as expected, much faster convergence can be observed for the former.

## V. Conclusions

We have presented some analytic results about the performance of the equalizer  $v[n]$  associated with the SEA as the equalizer order and data length are sufficient large. These analytic results demonstrate that the SEA is applicable for finite SNR regardless of whether the channel has zeros on the unit circle or not. This equalizer is stable with a nonlinear relation to the MMSE equalizer (see Properties 1 and 2) and capable of performing perfect phase equalization for the two cases mentioned in Property 3. A preferable choice of  $p$  and  $q$  is  $p = q = 2$  (see (7)) as the SEA is employed to process complex measurements. Both the SEA and the deconvolution criteria  $J_{p,q}$  given by (4) result in the same equalizer for the two cases mentioned in Property 3 as presented in Fact 1.

An FFT based algorithm, Algorithm 2, was presented to obtain the true  $v[n]$  from the channel and MMSE equalizer based on Property 1. A fast algorithm making use of the SEA, Algorithm 1, was presented for finding the equalizer  $v[n]$  associated with  $J_{p,q}$  due to Fact 1. Some simulation results were also presented to support the analytic results and Algorithms 1 and 2.

## VI. References

- [1] O. Shalvi and E. Weinstein, "New criteria for blind deconvolution of nonminimum phase systems (channels)," *IEEE Trans. Information Theory*, vol. 36, pp. 312-321, March 1990.
- [2] O. Shalvi and E. Weinstein, *Universal Methods for Blind Deconvolution*, A chapter in *Blind Deconvolution*, S. Haykin, ed., Prentice-Hall, Englewood Cliffs, New Jersey, 1994.
- [3] O. Shalvi and E. Weinstein, "Super-exponential methods for blind deconvolution," *IEEE Trans. Information Theory*, vol. 39, no. 2, pp. 504-519, March 1993.
- [4] C.-C. Feng and C.-Y. Chi, "Performance of cumulant based inverse filters for blind deconvolution," *IEEE Trans. Signal Processing*, vol. 47, no. 7, pp. 1922-1935, July 1999.
- [5] C.-C. Feng and C.-Y. Chi, "Performance of Shalvi and Weinstein's deconvolution criteria for channels with/without zeros on the unit circle," to appear in *IEEE Trans. Signal Processing*, Feb. 2000.
- [6] J.G. Proakis, *Digital Communications*, McGraw-Hill, New York, 1995.
- [7] C.-C. Feng, "Studies on cumulant based inverse filter criteria for blind deconvolution," Ph.D. Dissertation, Department of Electrical Engineering, National Tsing Hua University, Taiwan, R.O.C., June 1999.

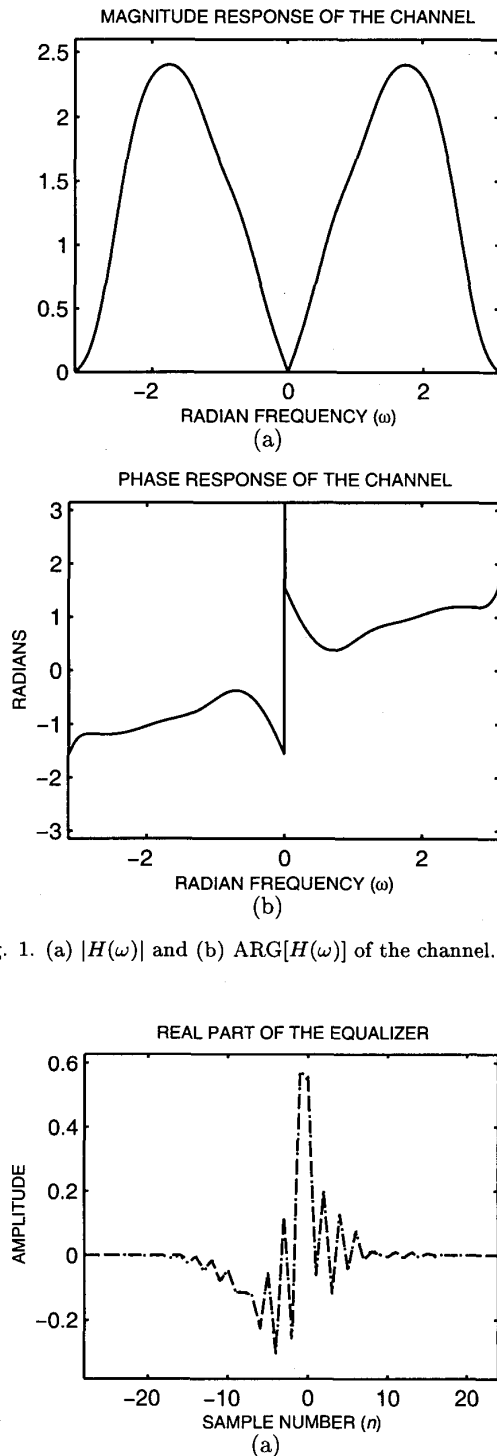


Fig. 1. (a)  $|H(\omega)|$  and (b)  $\text{ARG}[H(\omega)]$  of the channel.

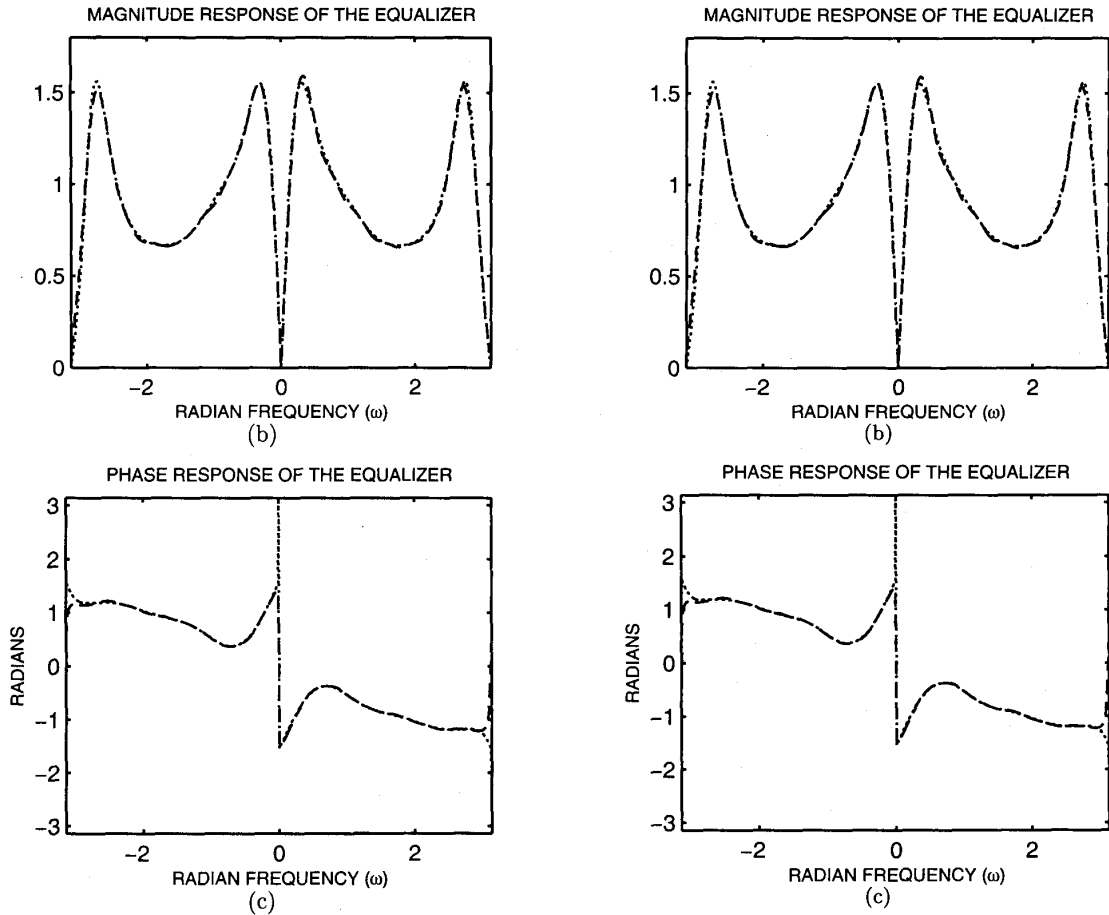


Fig. 2. Simulation results using the SEA. (a) Real parts, (b) magnitude responses and (c) phase responses of  $\hat{v}_{ave}[n]$  (dash lines) and the true  $v[n]$  (dotted lines).

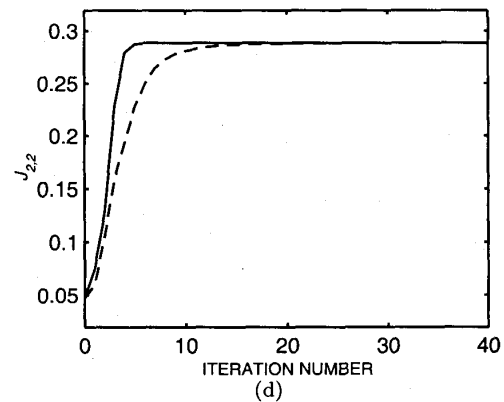
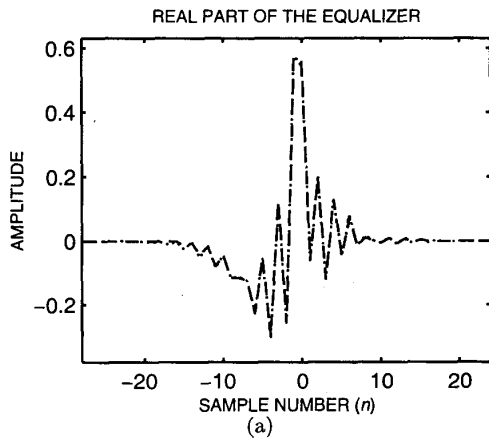


Fig. 3. Simulation results using  $J_{2,2}$ . (a) Real parts, (b) magnitude responses and (c) phase responses of  $\hat{v}_{ave}[n]$  (dash lines) and the true  $v[n]$  (dotted lines); (d) average of thirty  $J_{2,2}$ 's associated with Algorithm 1 (solid line) and that associated with a gradient-type algorithm (dash line).